



Human Activity Recognition for Elderly Care Using Light Gradient Boosting Machine (LGBM) Algorithm in Mobile Crowd Sensing Application

Erita Cicilia Febrianti¹ Amang Sudarsono^{1*} Tri Budi Santoso¹

¹*Department of Informatics and Computer Engineering, Politeknik Elektronika Negeri Surabaya, Indonesia*

* Corresponding author's Email: amang@pens.ac.id

Abstract: This paper focuses on human activity recognition (HAR) for elderly care using the Light Gradient Boosting Machine (LGBM) algorithm. HAR plays a vital role in monitoring and ensuring the well-being of older individuals. By analysing sensor data, this system can accurately detect activities such as jogging, walking, sitting, and standing. The proposed framework integrates LGBM with an Android application that reads user movement data, classifies activities, displays step counts per day, and provides rewards for achieving movement targets. To address privacy concerns, user data is anonymized using Elliptic Curve Cryptography (ECC) Blind Signature. The system leverages the power of artificial intelligence models in the Mobile Crowd Sensing (MCS) server to effectively distinguish between different activities with high accuracy and reliability. By remotely monitoring the elderly's activities, healthcare providers can ensure their safety. Experiment results show the practicality of proposed system by achieving overall accuracy of activity recognition when sitting, standing, walking, and jogging 97.5%.

Keywords: Human activity recognition, Mobile crowd sensing, LGBM, Blind signature, ECC.

1. Introduction

Recognizing human activity has long been a key component of Human-Computer Interfaces (HCI). Novel applications in healthcare, security, and entertainment are among the many areas that new ideas in human activity recognition (HAR) and sensing technologies aim to enable [1, 2]. Using a variety of technologies, including vision-based [3], acoustic-based [4], accelerometer-based [5], wearable sensors [6], environment-installed sensors [7, 8] and smartphones [9], a vast amount of literature has been presented in this crucial search field.

Human activity recognition plays a crucial role in elderly care, as it helps monitor and ensure the well-being of older individuals [10]. This technology utilizes a combination of artificial intelligence algorithms to accurately classify and identify various activities performed by elderly people. By analyzing sensor data techniques, this system can detect activities such as jogging, walking, sitting, standing [11, 12]. According to a 2011

World Health Organization (WHO) survey, over 650 million people of working age around the world are disabled [13]. There are currently insufficient facilities to accommodate the needs of people with disabilities [14, 15]. One of these is the need for a companion to supervise their activities. People with disabilities must be protected and supervised at all times to avoid injury, danger, or accidents [16].

Artificial intelligence is becoming more popular for HAR due to its self-learning capabilities and robust classification models [17]. In recent years, several studies on HAR have been conducted using machine learning and deep learning [18-20], but only a few have focused on developing a framework for the HAR system for the elderly. Kaixuan Chen et al. [21] provided an overview of the challenges and opportunities in the field of human activity recognition using deep learning techniques.

Activity recognition has become one of the due to the availability of various sensors available on smartphones and wearable sensors such as accelerometer, gyroscope, GPS and etc [22]. With the advancement of sensor technology and mobile

computing. Mobile Crowd Sensing (MCS) is a new breakthrough in IoT that has advantages in the process of acquiring sensor data from the surrounding environment. The availability of several sensors integrated with smartphones or wearable devices is one of the advantages of the MCS paradigm. In addition to several advantages, security and privacy [23-25] are of important in MCS systems. In MCS, users' personal information such as identity and location information are vulnerable to privacy attacks. Some kinds of attacks on MCS include Spoofing, Malware, Jamming, DoS, and etc [26-27]. Challenges to the security and privacy of user data are important in the process of implementing classification using a source that uses the MCS method, namely by adding security algorithms to the system.

So, in this paper the contribution is analyses with Light Gradient Boosting Machine (LGBM). LGBM is a development of the Gradient Boosting algorithm method [28]. In Gradient Boosting Decision Tree (GBDT), a decision tree model will experience the addition of the error experienced by the previous decision tree model, which is added to the training process. LGBM uses the same principle, but prefers tree-leaf based model building over level-wise, as a result LGBM models are prone to overfitting. However, the loss in this model can be kept as low as possible, where the error is suppressed by using a gradient-boosting algorithm. The modelling results of LGBM will be integrated with an Android application, which will read data from the movement of user activities, classify user activities, display step counts per day, and provide rewards for reaching the target movement in the form money coins according to the MCS scheme. The reward system will be provided by the ministry of health. The data obtained from sensor readings, along with the identity of the user such as NIK, name, age, gender, classification results will be converted to anonymous to disguise the privacy of user data using ECC Blind Signature. By utilizing the powerful capabilities of artificial intelligence models in the MCS server, this system can effectively distinguish between different activities performed by elderly individuals with high accuracy and reliability of security [29]. By accurately recognizing these activities, healthcare providers can remotely monitor the elderly [30, 31].

The remainder of this paper is divided into the following sections. Section 2 includes related works. The proposed system will be discussed in Section 3. The measurement result and discussions will be discussed in Section 4. The paper conclusion in Section 5.

2. Related works

Among the studies on mobile crowd sensing and human activity recognition are Csizmadia et.al [32] This paper presents a study investigating the use of wearable devices and machine learning to automatically recognize children's activities. The goal was to develop a reliable method for detecting 40 different playful and everyday activities that could form the basis of applications to facilitate physical activity or predict developmental disorders. 34 children ages from 6 to 8 years wore smartwatches equipped with motion sensors while performing the activities. A test battery called BATB was developed including activities like hopscotch, crawling, and everyday tasks. Motion data was collected and analysed using a Light Gradient Boosted Machine (LGBM), a decision tree-based machine learning algorithm. The LGBM model achieved an overall classification accuracy of 95% across all activities. To account for class imbalance, Area under the ROC Curve (AUC) scores were also reported and found to be above 0.8 for 17 out of the 40 activities, indicating very good recognition performance for many tasks. The AUC is a metric that quantifies the overall performance of a classification model. It represents the probability that a randomly chosen positive instance (e.g., a true positive) will be ranked higher than a randomly chosen negative instance (e.g., a false positive). Playful activities tended to yield higher AUC scores compared to everyday tasks, possibly because they involve more complex body patterns. Notably, the window size parameter, which defines the time interval of data used for classification, had no significant impact on performance across the range tested from 0.3 to 3 seconds. This suggests the method is robust to window size choice. Sample size did appear to influence results, with lower recognition for rarer activities. This study demonstrates the feasibility of using commodity wearable sensors and machine learning to automatically recognize a variety of children's physical activities with very good accuracy and AUC scores. The methods developed could enable new applications to promote activity in interactive games by providing real-time feedback. The ability to detect certain activities also has applications for screening developmental disorders. In summary, this paper presented a well-designed activity recognition study that achieved strong results for children's tasks using LGBM modelling. The methods developed have practical applications and provide guidance for further optimizing automated behaviour analysis through wearable devices and machine learning. In

this paper the model achieved an overall classification accuracy of 95%, so it can be reviewed if LGBM is suitable for active movements such as children's activities which later for our paper to classify activities for elderly people will achieve better accuracy.

Research carried out by Guolin Ke, et.al. [33]. In the AI model used in several intelligent systems, the majority of these systems use the Neural Network approach and also Deep Learning. As mentioned earlier, the Deep Learning model has a disadvantage in terms of high resource consumption, so additional techniques are needed for the suppression process, including compression or encoding techniques. Researchers consider the existence of other AI models that can be based on the way decision trees work, so they are called tree-based models. One example is the Gradient Boosting Decision Tree or GBDT. GBDT itself is a fairly popular model to implement, coupled with several variants of modifications to add optimization to the model, such as the Extreme Gradient Boosting (XGBoost) model, as well as the Gradient Boosted Regression Tree (GBRT). With the existence of various variants of tree-based models, researchers built a new model that has a faster processing speed compared to existing models (up to 20x faster), but can achieve the same level of accuracy. The proposed model combines the GBDT model with the Gradient-based One-Side Sampling (GOSS) technique as well as the Exclusive Feature Bundling (EFB) technique. This new model is called the Light Gradient Boosting Machine or LightGBM. Comparison of the processing speed of the LightGBM model. Where the results to achieve AUC 0.78, the LGBM model only takes 100 seconds, while other models take about 900-1000 seconds, which proves that LGBM works faster, even though the data has high sparsity and volume.

In other research Gao, et.al [34] This paper proposes a human activity recognition algorithm based on stacking denoising autoencoder (SDAE) and LightGBM (LGB). The SDAE is used to extract features from raw sensor data in an unsupervised manner, removing noise from the sensors. LightGBM is then used for the supervised classification of activities. The methodology has four main steps - data acquisition, preprocessing, unsupervised feature extraction via SDAE, and supervised classification with LightGBM. Smartphone sensors are used to collect data on human moving modes, static behaviours, and dynamic behaviours. The data is segmented into windows and standardized before feature extraction. SDAE is applied separately to each sensor stream to

learn features in an unsupervised layer-wise manner. Noise is added during training to make the network more robust. Extracted features from all sensors are concatenated to form the final feature vector. Analysis shows the SDAE reduces inner-class dispersion by 97.5% while increasing outer-class dispersion, improving separability. LightGBM is then used for classification. A boosting k-fold approach is proposed, where errors from one-fold are prioritized in the next fold's training, improving accuracy. The algorithm is evaluated on four public datasets with six activity classes are walk, walkup, walkdown, sit, stand, and lay. The results show an average accuracy of 95.99% across the four datasets, outperforming XGBoost (92.16%), CNN (93.52%), CNN with statistical features (97.63%), and single SDAE (97.9%). This demonstrates the proposed algorithm is effective for activity recognition from inertial sensors even with data from different devices and scenarios. In conclusion, this paper presents an activity recognition method based on stacking denoising autoencoder for unsupervised feature extraction and LightGBM for supervised classification. It achieves state-of-the-art average accuracy on multiple datasets, indicating robustness to data variations. The boosting k-fold approach also helps optimize LightGBM. Overall, the methodology effectively recognizes human activities from smartphone sensors. However, the addition of noise to user raw data, the problem of data training time and accuracy.

Research Zhang, et.al [35] This paper proposes a semi-supervised learning approach using LightGBM for human activity recognition based on smartphone sensors. It aims to improve the recognition accuracy and robustness with limited labeled data. A key contribution is the use of semi-supervised learning to enrich the dataset by leveraging a large amount of unlabeled data. The data was collected from 20 subjects performing 5 indoor activities (climbing stairs, stillness, walking, taking elevator/escalator) using smartphone sensors. After preprocessing and feature extraction from sliding windows, only 10% of the data was labeled for training, with the remaining 90% unlabeled. A graph-based label spreading algorithm was adopted for semi-supervised learning, achieving 97.94% labeling accuracy. LightGBM was then applied to the enriched dataset for classification and compared against other supervised and semi-supervised techniques. LightGBM was chosen due to its robustness from the histogram algorithm, GOSS sampling, EFB feature bundling, and leaf-wise learning strategy. The experimental results showed semi-supervised LightGBM achieved the best

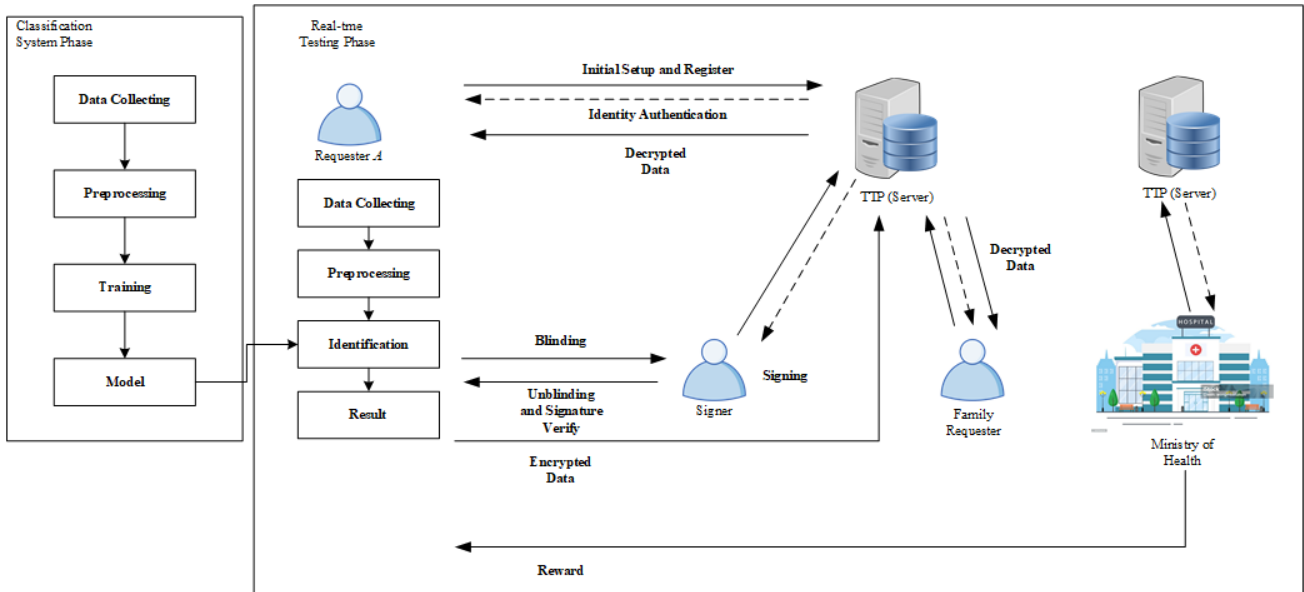


Figure. 1 Proposed Activity Recognition for Elderly in MCS

overall accuracy of 85.24%, outperforming the other supervised models (83.5-70.92%) and semi-supervised models. An analysis of the LightGBM confusion matrix showed highest f-score for climbing stairs activity recognition at 91.34% due to distinct sensor patterns, while stillness had the lowest at 81.35% due to minimal movements. Elevator/escalator recognition was similar to walking. The semi-supervised approach consistently outperformed supervised learning for all classifiers by enriching the dataset. In conclusion, the study presented an effective semi-supervised human activity recognition approach using LightGBM. By leveraging unlabeled data through label spreading, the dataset was enriched which improved generalization compared to limited labeled data alone. LightGBM proved robust for activity classification, achieving state-of-the-art accuracy of 85.24% on the dataset. The key advantages of the proposed methodology are its ability to improve recognition performance with limited labeling effort through semi-supervised learning and LightGBM's robustness. Just like the first research before, the 5 activities performed in this research resulted in an accuracy of 85.24% where the accuracy results for our research could be higher for elderly activities.

3. Proposed system

The proposed system integrates two main components: a machine learning scheme that uses the LightGBM algorithm for activity recognition and a secure blind signature that uses Elliptic Curve Cryptography (ECC). Additionally, users who successfully complete the activity requirements will receive rewards in accordance with the MCS

scheme. The reward system will be provided by the ministry of health. In LightGBM, we use a concept known as verdict trees, "verdict trees" refer to the decision trees used within the algorithm to make predictions. These decision trees are also known as "base learners" or "weak learners." The term "verdict" might imply that each tree is making a judgment or decision about the outcome based on the input features. In ensemble methods like gradient boosting, these verdict trees are combined to form a strong predictive model, so that we can cram a function such as, from the input space X , towards the gradient space G . It is assumed that there is a training set with instances like x_1, x_2 , and up to x_n , where each element is a vector in space X with s dimensions. All of the negative gradients of a loss function with regard to the output model are indicated as g_1, g_2 , and up to g_n , in each of the restatements of a gradient boosting. In actuality, the decision tree separates each node at the most explaining characteristic, which also produces the greatest evidence gain. With this kind of model, the variance following segregation can be calculated to determine how much the data has improved. It can be expressed by Eq (1):

$$Y = Base_tree(X) - lr \times Tree1(X) - lr \times Tree2(X) - lr \times Tree3(X) \quad (1)$$

Where Y is the dependent variable or the output of the equation, $Base_tree(X)$ represents the base tree function evaluated at X , lr is the learning rate, a scalar coefficient, $Tree1(X)$, $Tree2(X)$, and $Tree3(X)$ are functions representing the outputs of three different trees evaluated at X .

Explanation, let O be a training dataset on a fixed node of a decision tree and then the variance gain of dividing measure j at a point d for a node is defined as:

$$V_{j|O}(d) = \frac{1}{n_o} \left(\frac{\left(\sum_{\{x_i \in O: x_{ij} \leq d\}} g_i \right)^2}{n_{l|O}^j(d)} + \frac{\left(\sum_{\{x_i \in O: x_{ij} \geq d\}} g_i \right)^2}{n_{r|O}^j(d)} \right) \quad (2)$$

Where $n_o = \sum I[x_i \in O]$, $n_{l|O}^j(d) = \sum I[x_i \in O: x_{ij} \leq d]$, $n_{r|O}^j(d) = \sum I[x_i \in O: x_{ij} \geq d]$

Gradient One-Sided Sampling or GOSS utilizes every instance with a larger gradient and does the task of random sampling on the various instances with the small gradients. The training dataset is given by the notation of O for each particular node of the Decision tree. The variance gains of j or the dividing measure at the point d for the node is given by:

$$\tilde{V}_j(d) = \frac{1}{n} \left(\frac{\left(\sum_{x_i \in A_l} g_i + \frac{1-a}{b} \sum_{x_i \in B_l} g_i \right)^2}{n_l^j(d)} + \frac{\left(\sum_{x_i \in A_r} g_i + \frac{1-a}{b} \sum_{x_i \in B_r} g_i \right)^2}{n_r^j(d)} \right) \quad (3)$$

Where $A_l = \{x_i \in A: x_{ij} \leq d\}$, $A_r = \{x_i \in A: x_{ij} > d\}$, $B_l = \{x_i \in B: x_{ij} \leq d\}$, $B_r = \{x_i \in B: x_{ij} > d\}$, and the coefficient $\frac{1-a}{b}$ is used to normalize the sum of gradients over B back to the size of A^c .

The training phase and the testing phase are the two main stages of the machine learning scheme that uses supervised learning techniques. The input data is used in the training phase to establish the target, or corresponding output, and the classifier parameters, or training samples. As the Third Trusted Party (TTP) in the blind signature scheme, the server will produce as many keys as users—in this case, 100 users. Regarding the creation of public and private keys for the ECC algorithm utilizing curve secp384r1, which has a bit length of 384 bits and equation $y^2 \equiv x^3 - 3x + b \pmod{p}$, where parameter b which is 384 bits long with a bit length of 384 bits and $4a^3 + 27b^2 \neq 0$. Our blind signature protocol involves four participants: a family requester F , a signer B , and a requester A , and Ministry Health M . Next, in a role as a Third



Figure. 2 Map of Data Collection Location

Trusted Party (TTP), server S is in control of creating the system parameters and providing the user with a secure identity.

There are two scopes in our proposed scheme: a classification system phase and a real-time testing phase. There are eleven phases in the online scope: Initialization; identity verification; data collection; preprocessing; identification results; blinding phase, signing phase, unblinding phase and signature verification, encryption phase, decryption phase, and reward phase.

3.1 Classification system phase

To perform the classification process using artificial intelligence, the first step is to collect data from several users that will be used as input for the training process. The dataset has been created by involving 10 different users, who perform 4 types of movements namely sitting, standing, walking, and jogging.

A three-part data collection scenario was created for this research and includes the following:

1. A maximum 50 data points from sitting and standing activities will be sampled over a 1000 ms period, yielding 1 data point per second.
2. A maximum of 50 data points will be sampled during walking activities over a period, yielding 2 data points per second
3. A maximum of 50 data points will be sampled during the jogging activity over a 250 ms period, yielding 4 data points per second.

The dataset obtained will be pre-processed first so that it can be input for the artificial intelligence training process. Preprocessing includes filtering using IIR Filter, normalization using z-score, feature extraction on each sensor and axis so that 24 features are obtained, training and tuning of artificial intelligence modelling that will be used. There are several AI models that will be tested using the dataset to compare the accuracy of the system and also the computation time that needs to be done by the system on the incoming data.

Eq (3) can be used to calculate the Low Pass process utilizing an IIR filter.

$$H(z) = \frac{b_0 + b_1 z^{-1} + \dots + b_n z^{-m}}{1 + a_1 z^{-1} + \dots + a_n z^{-m}} \quad (3)$$

The equation of z-score can be calculated in Eq. (4):

$$Z = \frac{x - \mu}{s} \quad (4)$$

Where s is the attribute population's standard deviation, μ is the attribute population's average, and x is the raw data.

3.2 Real-time testing phase

In testing artificial intelligence, the help of an Android application that can read Accelerometer and Gyroscope sensor data from a user activity will be used. By using an artificial intelligence model that has been trained, the user's reading condition will be classified whether it is included in the activity of sitting, standing, walking, or jogging. The sensor reading data is added with the user's location to show the user's location. In the real-time testing phase, the user registers first, after which the server authenticates the user, allowing the user to record their activities. The Android then classifies their activities, and the model derived from the training results is compared in real time with the feature extraction results. After the user records the activity of walking and jogging counting every 10 minutes, the user will be rewarded with a coin of 10 rupiah. Giving rewards is done so that users have the enthusiasm to do walking and jogging activities. Moreover, data encryption and blind data collection are done.

- a. *Initialization.* To configure the system, we specify the domain's parameters during registration. This includes creating an elliptic curve $E(Fq)$, over a prime field Fq with q exceeding 384 bits. An order d and base point G are chosen on the curve. The server generates a public-private key pair, with the public key $Pk_S = n_s \cdot G$. Users select their private keys and generate their public keys. Registration on the server is required before accessing services. Users receive a JSON Web Token (JWT) for authentication. Each user is provided with a unique set of keys, sent securely from the server.
- b. *Identity Verification.* After registration, user authentication is performed to allow access to valid users and prevent unauthorized access. The authentication process involves generating a

JSON Web Token (JWT) for each registered user. The JWT serves as a token that can be used to verify the user's identity and grant access to the system.

- c. *Data Collecting.* Data collection in real-time testing process involves obtaining raw data from accelerometer and gyroscope sensors. The raw data includes 3 values (x, y, z) from the accelerometer and 3 values (ϕ, θ, ψ) from the gyroscope. The collected data is unlabelled and used as input for preprocessing.
- d. *Preprocessing.* Data preprocessing in the real-time testing process involves three stages: filtering, feature extraction, and normalization. The pre-processed data is then used as input for machine learning identification in an Android application.
- e. *Identification Result.* In the decision-making stage, the normalized data is used as input to predict activities using a loaded model. The model compares the input data and generates predictions for each activity.
- f. *Blinding Phase.* Blindness is primarily used for protecting communications without the signer's knowledge. Requester A uses their public and private keys (n_A, Pk_A), along with the message digest $h(m)$ and hash of ID user $h(ID)$ to blind the message $m = h(m) \parallel h(ID)$. The blinding operation is computed according to $\alpha = m \cdot n_A \cdot Pk_A$, resulting in the blinded message α . This blinded message is then received by the signer B and other family requesters F' .
- g. *Signing Phase.* Upon receiving the message α , the signer B and other family requester F' select random integers β in the range $[2, d - 2]$. They use these integers to calculate the secret elements $R_B = \beta_B \cdot \alpha$ and $R_{F'} = \beta_{F'} \cdot \alpha$, and the blind signatures S as $S_B = (n_B + \beta_B) \cdot \alpha$ and $S_{F'} = (n_{F'} + \beta_{F'}) \cdot \alpha$. The message signature pairs $(\alpha, (R, S))$ are then sent back to the requester A .
- h. *Unblinding and Verification Phase.* To reveal the blind signature, Requester A uses the blind signature S_B , the previously generated message 'm', private key n_A , and the public key Pk_B of the signer. This allows extracting the blind signature $S_{B'}$ using $S_{B'} \equiv S_B - m \cdot n_A \cdot Pk_B$. The same process is applied for the other family requester F' , as expressed $S_{F'} \equiv S_{F'} - m \cdot n_A \cdot Pk_{F'}$. Requester A also computes the message digest value m' and performs the unblinding process according $m' \equiv n_A \cdot (n_A - 1) \cdot m + m$. Requester A then verifies the authenticity of the signature and the transmitted message digest using the signer's public key Pk_B and the public keys $Pk_{F'}$
- i. $S_{B'}$ using $S_{B'} \equiv S_B - m \cdot n_A \cdot Pk_B$. The same process is applied for the other family requester F' , as expressed $S_{F'} \equiv S_{F'} - m \cdot n_A \cdot Pk_{F'}$. Requester A also computes the message digest value m' and performs the unblinding process according $m' \equiv n_A \cdot (n_A - 1) \cdot m + m$. Requester A then verifies the authenticity of the signature and the transmitted message digest using the signer's public key Pk_B and the public keys $Pk_{F'}$

Table 1. Samsung A54 Specifications

Samsung A54 Specifications	
Processor	Exynos 1380
Android Version	Android 13, One UI 5.1
Random Access Memory (RAM)	6 GB
Connectivity	Wi-Fi 802.11 a/b/g/n/ac, dual-band, Wi-Fi Direct, hotspot

of other family requesters. The validity $R_B.Pk_B \stackrel{?}{=} S_{B'} - m'.Pk_B$ and $R_{F'}.Pk_{F'} \stackrel{?}{=} S_{F'} - m'.Pk_{F'}$ is checked during this verification process.

- j. *Encryption Phase.* The encryption phase aims to prevent unauthorized access to sensitive information during data transfer. Measures like data segmentation, padding, and encryption algorithms (such as AES-CBC) are employed to enhance operational security. The resulting encrypted data is stored in the database.
- k. *Decryption Phase.* Decryption is the process of converting encrypted messages back to their original state. On an Android device, decryption is performed to display the results of user activity classification by Requester *A* and Requester Family *F*. The ciphertext block C_i is decrypted using the decryption function with the same key k , and the plaintext block v_i is derived using the intermediate value IV_i and the previous ciphertext block c_{i-1} . If padding was added during encryption, it is removed to recover the original plaintext.
- l. *Reward Phase.* The reward phase is conducted by the Ministry of Health *M*. This reward is given to users who have done walking and jogging activities for 10 minutes with a reward of 10 rupiahs.
 $S \rightarrow R_1, Activity.RESULT_OK, data \rightarrow U$
 Where S be the starting of retrieving activity recognition. Let $R_{i,j,k}$ represents the invocation with request code i , result code j , and data k . Let U be the update of obtained coins.

4. Measurement result and discussion

In this section, we discuss about the classification system phase and real-time testing result phase. The outcomes of machine learning training using accelerometer and gyroscope sensors are shown in the classification system phase. The results of the blind signature using the ECC algorithm and the model's testing from the training results are displayed in the classification system phase.

4.1 Classification system result

The first step is collecting raw data from Accelerometer sensors (x, y, z) and Gyroscope sensors (ϕ, θ, ψ), up to 50 data points per axis, using an application that has been customized with varying time intervals based on the user's activities. There are 200 total data points that are used in the training process. One time with a smartphone (Samsung Galaxy A54) placed on the right thigh. Samsung A54 specifications can be seen in Table 1. To reduce noise using IIR Filter with 25Hz cutoff frequency applied. After reduce noise is feature extraction, resulting in 24 extracted features that are ready to be used for machine learning as a better separable representation of the raw sensor data. The following shows in Fig. 3 the results of plot box feature extractions on each activity. Although extracted features may not appear perfectly separable, a machine learning model can accurately classify activities by combining multiple features. Figs. 1(a)-(d) show box plots grouped by activity. In sitting activity, we look at the range of mean x values, the sitting activity has the lowest range of values, indicating the most limited movement while sitting. The standard deviation of x for the sitting activity also has the lowest range of values, indicating high stability of movement while sitting. The maximum and minimum values of x for sitting activities also have the lowest range of values, indicating the most restricted movement while sitting. Standing Activity, we look at the range of mean x values, standing activities have a slightly higher range of values than sitting, indicating less variation in movement while standing. The standard deviation of x for standing activities also has a slightly higher range of values than sitting, indicating a slight variation in movement while standing. The maximum and minimum values of x for standing activities also have a slightly higher range of values than sitting, indicating there is little variation in movement while standing. Walking Activity we look at the range of mean x values, walking activity has an even higher range of values than sitting and standing, indicating more movement than sitting or standing. The standard deviation of x for walking also has a higher range of values, indicating a greater variation in movement when walking. The maximum and minimum values of x for walking also have a higher range of values, indicating a wider range of movement when walking. Jogging Activity, we look at the range of mean x values, the jogging activity has the highest range of values, indicating the most intense and extensive movement compared to the other activities. The

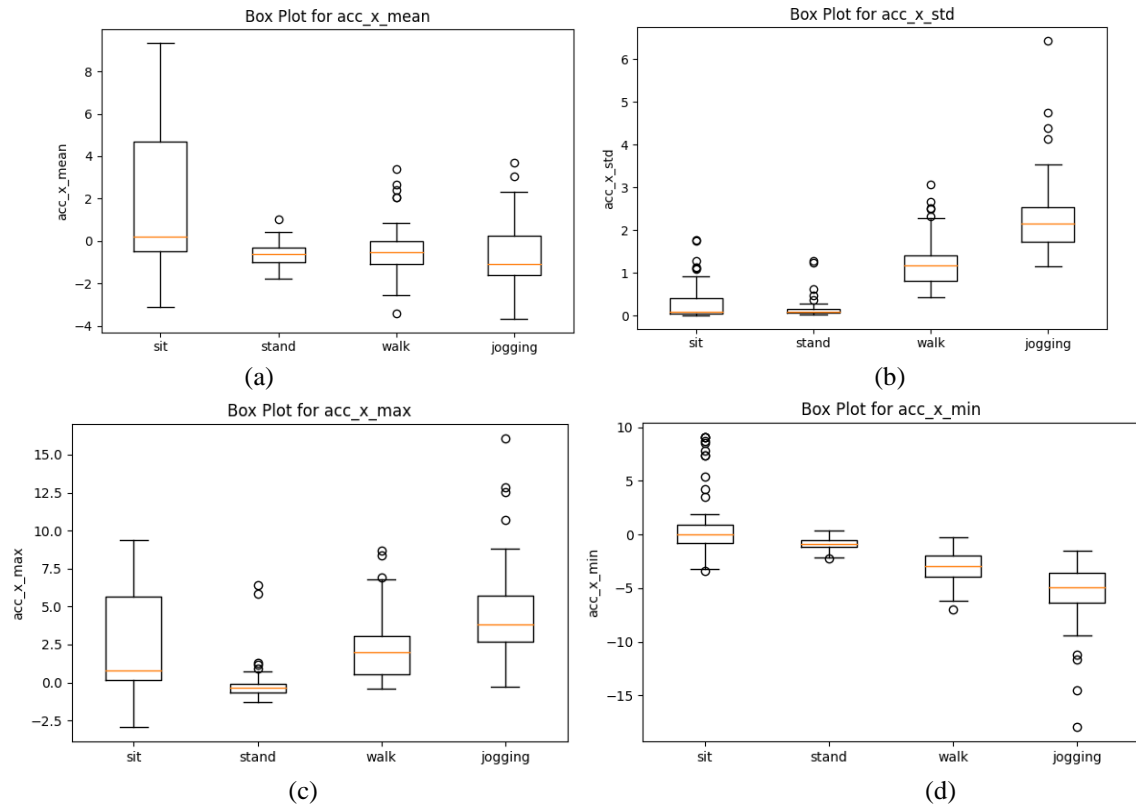


Figure. 3 Box plots for four features of the dataset grouped by activity: (a) mean of the x -axis signal accelerometer, (b) standard deviation of the x -axis signal accelerometer, (c) max of the x -axis signal accelerometer, and (d) min of the x -axis signal accelerometer

Table 2. LightGBM Tuning Parameters

Parameter	Value
objective	multiclass
num_class	4
boosting_type	gbdt
metric	multi_logloss
learning_rate	0.05
feature_fraction	0.9
bagging_fraction	0.8
bagging_freq	5

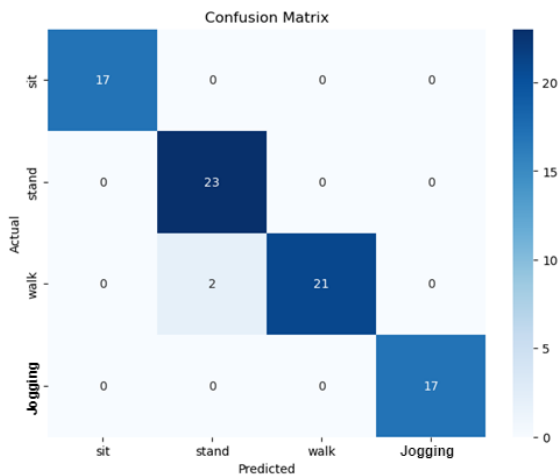


Figure. 4 Confusion Matrix

standard deviation of x for the jogging activity also has the highest range of values, indicating the greatest variation in movement and instability compared to the other activities. The maximum and minimum values of x for the jogging activity also have the highest range of values, indicating the most extensive and intense movement compared to the other activities. The next step is the normalization process, which employs the z-score technique. After that the data collecting, preprocessing and feature extraction, and normalization necessary to get reasonable results from machine learning is already done by the HAR Smartphone dataset. First, to comprehend the dataset, various plots are used, such as box plots per activity to understand feature distribution for various activities. Finding the ideal number of features to best represent the data is the next step, since the dataset contains 24 extracted features. For this we use some of the LightGBM parameters in Table 2. Parameter explanations are as follows: objective, the objective parameter specifies the loss function to be optimized during the training of the gradient boosting model. In this case, the "multiclass" objective is selected, indicating that the model will be trained for multiclass classification tasks. num_class, this parameter specifies the number of classes in the multiclass classification

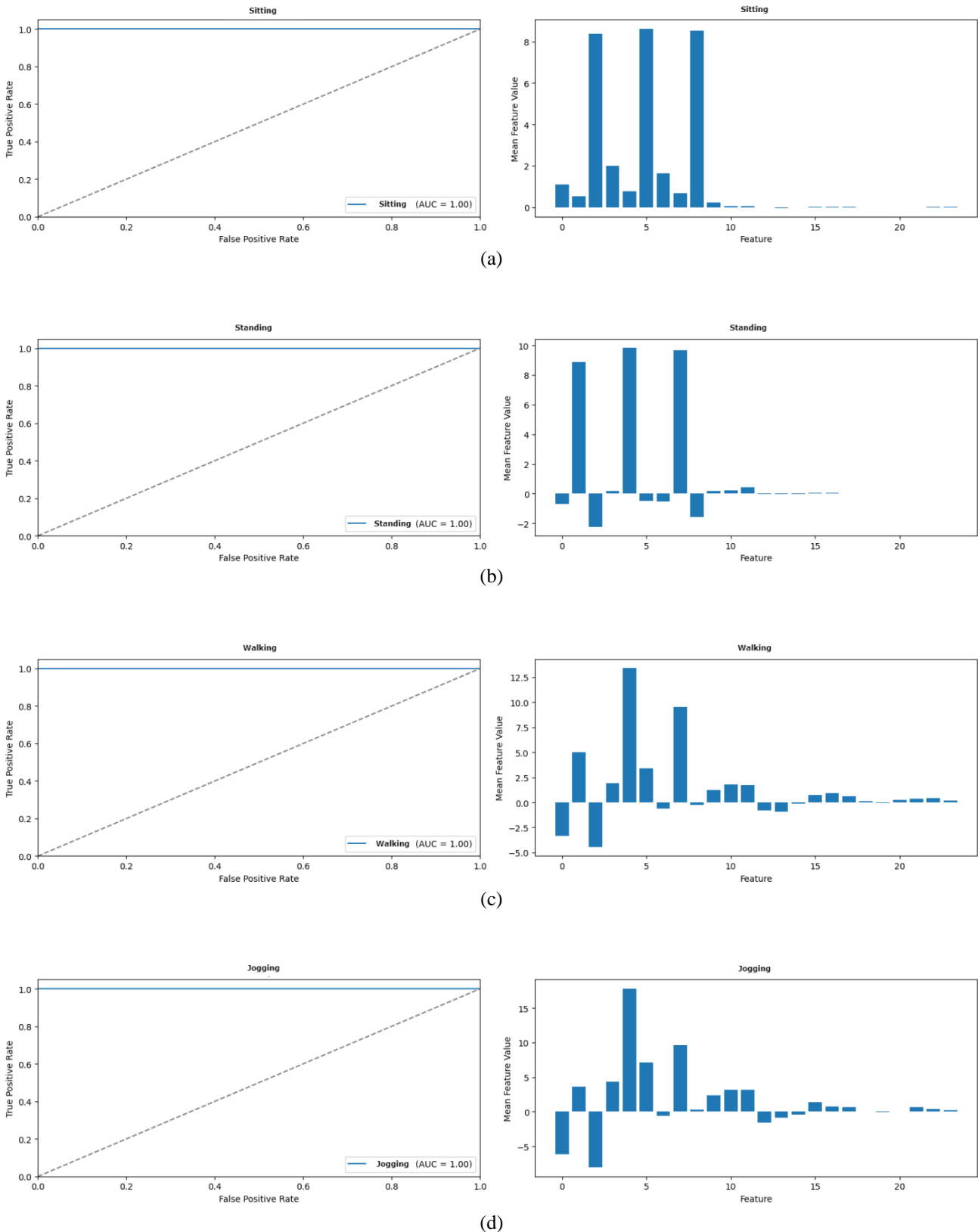


Figure. 4 AUC Values: (a) AUC Values in sitting activity, (b) AUC Values in standing activity, (c) AUC Values in walking activity, and (d) AUC Values in jogging activity

problem. In this paper, the value is set to 4, indicating that there are four classes to be predicted. Boosting_type, the boosting_type parameter determines the type of boosting algorithm to be used.

In this case, "gbdt" (Gradient Boosting Decision Tree) is selected. GBDT is a popular boosting algorithm that builds an ensemble of decision trees sequentially, where each subsequent tree corrects

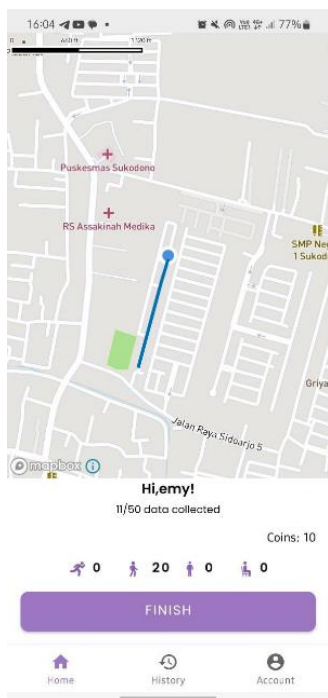


Figure. 5 Visualization in Walking Activity

Table 3. Metric Evaluation of Each Class [36]

Class	Precision	Recall	f1-score	Support
Sit	1	1	1	17
Stand	0.92	1	0.96	23
Walk	1	0.91	0.95	23
jogging	1	1	1	17
Overall accuracy	0.975			

the mistakes made by the previous ones. metric: The metric parameter specifies the evaluation metric to be used during training. In this case,

"multi_logloss" is selected, which is the logarithmic loss function for multiclass classification. It measures the performance of the model based on the predicted probabilities for each class. Learning_rate, the learning_rate parameter determines the step size at each iteration of the gradient boosting algorithm. It controls the contribution of each tree in the ensemble. A lower learning rate can make the model generalize better but may require more iterations to converge. feature_fraction, this parameter controls the fraction of features (randomly selected) to be used in each tree. It helps in reducing overfitting by introducing randomness and forcing the model to consider different subsets of features. Bagging_fraction. The bagging_fraction parameter specifies the fraction of training data to be randomly sampled (with replacement) for each iteration. It helps in reducing overfitting by introducing diversity in the training process. Bagging_freq, this parameter determines the frequency of bagging. It specifies the number of iterations before a bagging process is performed. Bagging is the process of training each tree on a different subset of the data to further introduce diversity and reduce overfitting. We use comparison of 60% training data and 40% testing data, displaying the findings of testing the classification model's performance on both the original (ground truth) and predicted data, as represented by the confusion matrix in Fig. 4. All of the activities had at least acceptable AUC values, and the majority had very good values, e.g. four activities were recognized with AUC values of 1. The outcomes were attained with a testing accuracy of 97.5% based on confusion matrix data. Table 3 displays the detailed results metric evaluation from the first trial, with calculations and evaluations for each class.

Table 4. Performance Comparison of The Proposed Scheme and Four Existing Similar Research

Goals	Csizmadia et.al [32]	by Guolin Ke, et.al. [33]	Gao, et.al [34]	Zhang et.al [35]	Our Scheme
Good Accuracy	√ (accuracy 95%)	√ (Not Described)	√ (accuracy 92.16%)	√ (accuracy 85.24%)	√ (accuracy 97.5%)
Good AUC	√ (0.8)	√ (0.78)	NA	NA	√ (1)
Good Classification Time	NA	NA	NA	NA	√ (around 1 ms)
Blindness	NA	NA	NA	NA	√
Untraceability	NA	NA	NA	NA	√
Confidentiality	NA	NA	NA	NA	√
Correctness	NA	NA	NA	NA	√
Integrity	NA	NA	NA	NA	√
Nonrepudiation	NA	NA	NA	NA	√
Unforgeability	NA	NA	NA	NA	√

4.2 Real-time testing result

The validated model is then put to the test using real-time data from accelerometer and gyroscope sensors in the real-time testing phase. In this testing process, the phases of data preprocessing and collection are identical to those of machine learning-based data modelling. The normalization results will be used as input for activity prediction against the loaded model during the decision-making stage. In order for the model to generate output predictions for each activity, it will be compared to the input data. For computational cost are needed from data collecting until blind signature process is 12 seconds. the result of the computation cost is relatively short. This shows that the prediction system can work in real-time. Due to the fast classification computation time, there is no need to worry about losing data for further activities.

The next is the outcome of the blind signature ECC. The difficulty of solving the blind signature ECC establishes the resilience of our technique. In addition, the application of the blind signature approach enhances the general security of data transfers. The suggested scheme is enhanced and rendered more valuable for a range of uses by adding extra features in addition to the fundamental ones of blindness and untraceability, such as confidentiality, correctness, integrity,

nonrepudiation, and unforgeability. We examine these security requirements in the following manner for our plan.

Blindness, Blindness in signing refers to the inability of the signer to view the message's content while signing. Our method generates a blinded message, α , as $\alpha = m \cdot n_A \cdot Pk_A$. Without m (message digest) and the blinding factor ($n_A \cdot Pk_A$), neither the signer (B), nor other family requesters (F'), nor opponents can deduce the message (α). This blinding scheme relies on elliptic curve computation, making it challenging to decipher desired points in Blind Signature ECC. The process of inverting a hash function with parameter value m is complex, ensuring signer and requester sign the blinded message without content knowledge, fulfilling the blindness property effectively.

Untraceability, in any blind signature system, maintaining untraceability is essential. Once the message-signature pair becomes public, the signer can't link it back. Signer B , during signature request, only uses private key n_B and randomly generated β_B . This preserves untraceability, relying on secret factors like unique message digest m and A's private key n_A from Requester A, Signer B , and other Family Requester F' .

Confidentiality, entails concealing message contents from unauthorized entities. In this study, Requester A blinds messages, followed by signing by Signer B and other family Requester F' , and permutation before returning to Requester A. Intercepted texts pose a formidable challenge for decoding due to the Blind Signature ECC's complexity, effectively safeguarding message contents.

Correctness, ensures proper authentication of signatures with the Signer's public key. However, public verification might reveal the Signer's identity, compromising secrecy. Requester A verifies Signer B and Family Requester F' signatures using their public keys, ensuring correctness. Authentication relies on secret values derived from private keys, effectively maintaining correctness in the proposed framework.

Integrity, ensures data remains unchanged during transmission, thwarting malicious alterations. Tampering with specific data segments, like blind text sections, proves challenging due to their interdependence within encoded text. Altering a message triggers an avalanche effect, yielding vastly different outcomes, preserving integrity.

Nonrepudiation, ensures a signer cannot deny their signature on a legitimately signed message. Signer B electronically signs the blinded message, and their signature, along with user tracking, is returned to Requester A. Utilizing private keys and random numbers, B cannot refute signing, ensuring nonrepudiation. Requester A confirms legitimacy through signature validation, maintaining nonrepudiation effectively.

Unforgeability, ensures that only the legitimate signer can produce valid signatures for a given message within the allowed signing instances. Even if intercepted, adversaries cannot generate valid signatures without the signer's private key. With minimal likelihood of guessing valid signatures, the proposed method effectively maintains unforgeability through signature verification and cryptographic challenges.

The distinctive features are consistent with blind signatures, and we have described in detail the complex security requirements of our suggested scheme. A comparison of four comparable previous studies can be found in Table 4. In the table, a "✓" symbol denotes the fulfilment of a security requirement, whereas a "NA" or Not Available symbol indicates that the requirement has not been fulfilled in its entirety. The comparison demonstrates how the above goals of our current approach led to improved security in similar blind signature applications. Notably, our proposed

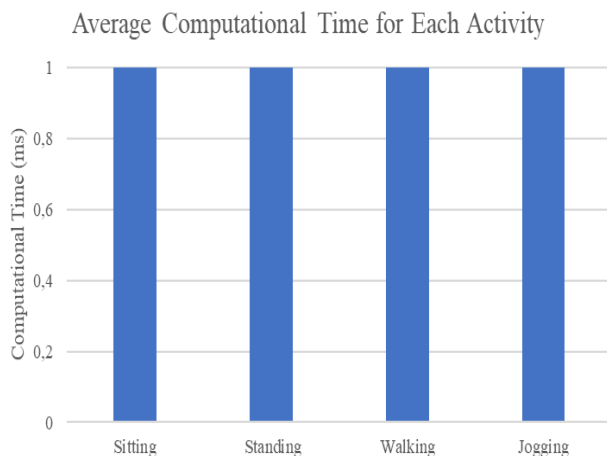


Figure. 6 Graph of Average Real-Time Classification Performance in Each Activity

scheme stands out for its enhanced security, while successful existing schemes have limitations in areas like blindness, untraceability, and correctness.

Table 4 shows how our proposed approach contributes to fulfilling the need for an authentication system that maintains machine learning accuracy values while preserving anonymity and privacy. For real-time classification performance run on smartphones, it consumes only about 1 ms in average. The real-time classification run on smartphones is shown in Fig. 6, from data input into the model to decision-making. With an average classification computation time of 1 ms, it is possible to derive the conclusion that the classification process begins with the model's data input and continues quickly until a decision is made. This demonstrates the real-time functionality of the prediction system. For subsequent activities, there is no need to be concerned about data loss due to the quick classification computation time. In research [32], the article presents a study utilizing wearable devices and machine learning to automatically recognize children's activities, aiming to facilitate physical activity promotion and predict developmental disorders. The study involved 34 children aged from 6 to 8 years wearing smartwatches equipped with motion sensors while performing 40 different activities. Motion data was analysed using a Light Gradient Boosted Machine (LGBM) algorithm, achieving an impressive overall classification accuracy of 95% across all activities. AUC scores, indicating recognition performance, were above 0.8 for 17 activities, particularly high for playful activities. Interestingly, the choice of window size for data classification had no significant impact on performance. However, recognition rates were lower for rarer activities,

indicating some influence of sample size. The study demonstrates the feasibility of using wearable sensors and machine learning for activity recognition in children, with potential applications in interactive games and developmental disorder screening. The robustness and practical implications of the method suggest its potential for further optimization and application, including potential use for classifying activities in elderly populations with anticipated improved accuracy. In research [33] The article discusses a new AI model, Light Gradient Boosting Machine (LightGBM), which combines Gradient Boosting Decision Tree (GBDT) with techniques like Gradient-based One-Side Sampling (GOSS) and Exclusive Feature Bundling (EFB). LightGBM achieves faster processing speeds (up to 20x) compared to existing models, maintaining high accuracy (AUC 0.78) even with sparse and

voluminous data, making it a promising alternative to resource-intensive deep learning approaches. In research Gao et al [34]. propose an activity recognition algorithm combining Stacking Denoising Autoencoder (SDAE) for unsupervised feature extraction and LightGBM (LGB) for supervised classification. The method achieves a state-of-the-art average accuracy of 95.99% across four datasets, outperforming other approaches. The boosting k-fold technique enhances LightGBM performance, demonstrating robustness across varied data scenarios from smartphone sensors. However, challenges such as data noise and training time persist. In research Zhang et al. propose a semi-supervised approach for human activity recognition using LightGBM and smartphone sensors. Leveraging limited labelled data and a large pool of unlabelled data, the method achieves 97.94% labelling accuracy with LightGBM, outperforming other models. The semi-supervised strategy consistently enhances recognition accuracy, reaching 85.24%. In [32-25] the datasets used are different, but the activities compared and the scenarios we propose are the same. Where the activity performed by [32-35] has the same activity that is compared to our work. In addition, the papers likely employ similar methodologies in terms of data collection, preprocessing, feature extraction, and machine learning techniques. For evaluation metrics, to assess the performance of their proposed methods, the papers may use common evaluation metrics such as accuracy, precision, recall, F1 score, or area under the curve (AUC). These metrics provide a standardized way to compare the effectiveness of different algorithms in recognizing human activities.

5. Conclusion

In conclusion, this paper focused on the development of a human activity recognition (HAR) system for elderly individuals using the Light Gradient Boosting Machine (LGBM) algorithm. The aim was to accurately classify and identify various activities performed by the elderly to monitor their well-being and provide remote healthcare services especially for elderly. The proposed system integrated the LGBM model with an Android application that collected sensor data from user movements, classified the activities, displayed step counts, and rewarded users for achieving movement targets based on the Mobile Crowd Sensing (MCS) scheme. The study highlighted the importance of HAR in elderly care, considering the increasing population of elderly individuals and the lack of sufficient facilities to meet their needs. By accurately recognizing activities such as jogging, walking, sitting, and standing. The overall classification accuracy of the system was 97.5% with AUC is 1, the system could contribute to ensuring the safety and supervision of individuals with disabilities, reducing the risk of injury or accidents. Artificial intelligence (AI) models, particularly LGBM, were identified as powerful tools for HAR due to their self-learning capabilities and robust classification models. While previous studies have focused on HAR using machine learning and deep learning techniques, this paper emphasized the need for a framework specifically tailored to the elderly population. The integration of LGBM with the Android application provided an effective solution for activity recognition and monitoring. Privacy and security concerns in MCS systems were addressed by implementing security algorithms and utilizing ECC Blind Signature to anonymize user data, protecting their identity and personal information. By ensuring the accuracy and reliability of security measures, healthcare providers could remotely monitor elderly individuals with confidence. The related works section discussed studies that further supported the feasibility and effectiveness of using wearable devices, machine learning, and tree-based models like LGBM for activity recognition. These studies demonstrated high classification accuracy and recognition performance, highlighting the potential applications in promoting physical activity, predicting developmental disorders, and optimizing behaviour analysis. In summary, this paper presented a comprehensive analysis and implementation of an HAR system for the elderly using the LGBM algorithm. The proposed system showcased

promising results in accurately classifying activities, monitoring step counts, and providing rewards based on movement targets. By leveraging AI models and MCS technology, the system offered a practical solution for remote healthcare monitoring of elderly individuals, contributing to their well-being and safety. Future research could focus on further optimizing the system, expanding the range of recognized activities, and conducting real-world evaluations to assess its effectiveness and usability in a practical setting.

Notations and Descriptions

$E (Fq)$	An elliptical curve E over a finite field Fq
G	A base point of elliptic curve
d	A prime order of G
Pk_S, n_S	A public and private key pair from Server
Pk_A, Pk_B, Pk_F	All users' public keys as requester (A), signer (B), and Family Requester (F)
n_A, n_B, n_F	All users' private keys as requester (A), signer (B), and Family Requester (F)
idA, idB, idF	User identity data, including requester (A), signer (B), and Family Requester (F)
m	a hash value obtained from the sequence of ciphertext
α	A blinded message
β	A random integer number
$R_B, R_{F'}$	Secret Element Signer B, Secret Element Other Family Requester
$S_B, S_{F'}$	Blind Signature Signer B, Blind Signature Other Family Requester
C_i	Ciphertext block
c_{i-1}	Previous ciphertext block
IV_i	Intermediate value

Conflicts of Interest

Authors declare no conflict of interest.

Author Contributions

The paper was conceptualized, implemented, collecting data, and documentation was completed by Erita Cicilia Febrianti. Amang Sudarsono and Tri Budi Santoso examined the work, offered recommendations and confirmed the outcomes.

Acknowledgments

This work was supported in part by the Ministry of Education, Culture, Research, and Technology of Indonesia, through Penelitian Dasar (Penelitian Tesis Magister) Scheme, 2024.

References

- [1] O. D. Lara and M. A. Labrador, "A Survey on Human Activity Recognition using Wearable Sensors", *IEEE Communications Surveys & Tutorials*, Vol. 15, No. 3, pp. 1192–1209, 2013.
- [2] Liming Chen, J. Hoey, C. D. Nugent, D. J. Cook, and Zhiwen Yu, "Sensor-Based Activity Recognition", *IEEE Transactions on Systems, Man, and Cybernetics, Part C (Applications and Reviews)*, Vol. 42, No. 6, pp. 790–808, 2012.
- [3] M. Siddiqi, R. Ali, Md. Rana, E. K. Hong, E. Kim, and S. Lee, "Video-Based Human Activity Recognition Using Multilevel Wavelet Decomposition and Stepwise Linear Discriminant Analysis", *Sensors*, Vol. 14, No. 4, pp. 6370–6392, 2014.
- [4] J. M. Sim, Y. Lee, and O. Kwon, "Acoustic Sensor Based Recognition of Human Activity in Everyday Life for Smart Home Services", *International Journal of Distributed Sensor Networks*, Vol. 11, No. 9, pp. 679123, 2015.
- [5] C. Torres-Huitzil and A. Alvarez Landero, "Accelerometer-Based Human Activity Recognition in Smartphones for Healthcare Services", *Springer Series in Bio-/Neuroinformatics*, pp. 147–169, 2015.
- [6] F. Attal, S. Mohammed, M. Dedabrishvili, F. Chamroukhi, L. Oukhellou, and Y. Amirat, "Physical Human Activity Recognition Using Wearable Sensors", *Sensors*, Vol. 15, No. 12, pp. 31314–31338, 2015.
- [7] V. Parra, V. López, and M. S. Mohamad, "A multiagent system to assist elder people by TV communication", *ADCAIJ: Advances in Distributed Computing and Artificial Intelligence Journal*, Vol. 3, No. 2, pp. 10–16, 2014.
- [8] D. Hernández De La Iglesia, G. Villarrubia González, A. López Barriuso, Á. Lozano Murciego, and J. Revuelta Herrero, "Monitoring and analysis of vital signs of a patient through a multi-agent application system", *ADCAIJ: Advances in Distributed Computing and Artificial Intelligence Journal*, Vol. 4, No. 3, pp. 19–30, 2016.
- [9] M. Shoaib, S. Bosch, O. Incel, H. Scholten, and P. Havinga, "A Survey of Online Activity Recognition Using Mobile Phones", *Sensors*, Vol. 15, No. 1, pp. 2059–2085, 2015.
- [10] H. Wang, J. Zhao, J. Li, L. Tian, P. Tu, T. Cao, Y. An, K. Wang, S. Li, "Wearable Sensor-Based Human Activity Recognition Using Hybrid Deep Learning Techniques", *Security and Communication Networks*, Vol. 2020, pp. 1–12, 2020.
- [11] C. Wang and Z. Peng, "Deep Learning Model for Human Activity Recognition and Prediction in Smart Homes", In: *Proc. of 2020 International Conference on Intelligent Transportation, Big Data & Smart City (ICITBS)*, pp. 741–744, 2020.
- [12] Z. Malki, E. Atlam, G. Dagnew, A. R. Alzighaibi, E. Ghada, and I. Gad, "Bidirectional Residual LSTM-based Human Activity Recognition", *Computer and Information Science*, Vol. 13, No. 3, pp. 40, 2020.
- [13] W. Bank, "World report on disability", *World Health Organization*, Vol. 91, pp. 549, 2011.
- [14] Du, Lim, and Tan, "A Novel Human Activity Recognition and Prediction in Smart Home Based on Interaction", *Sensors*, Vol. 19, No. 20, pp. 4474, 2019.
- [15] I. A. Bustoni, I. Hidayatulloh, A. SN, and N. G. Augoestin, "Multidimensional Earcon Interaction Design for The Blind: a Proposal and Evaluation," In: *Proc. of 2018 International Seminar on Research of Information Technology and Intelligent Systems (ISRITI)*, pp. 384–388, 2018.
- [16] S. Chernbumroong, S. Cang, A. Atkins, and H. Yu, "Elderly activities recognition and classification for applications in assisted living", *Expert Systems with Applications*, Vol. 40, No. 5, pp. 1662–1674, 2013.
- [17] T. H. C. Nguyen, J. C. Nebel, and F. Florez Revuelta, "Recognition of Activities of Daily Living with Egocentric Vision: A Review", *Sensors*, Vol. 16, No. 1, pp. 72, 2016.
- [18] C. Dhiman and D. K. Vishwakarma, "A review of state-of-the-art techniques for abnormal human activity recognition", *Engineering Applications of Artificial Intelligence*, Vol. 77, pp. 21–45, 2019.
- [19] G. Cheng, Y. Wan, A. N. Saudagar, K. Namuduri, and B. P. Buckles, "Advances in human action recognition: A survey", arXiv preprint arXiv:1501.05964, 2015.
- [20] D. Saraswathi and E. Srinivasan, "Performance analysis of mammogram CAD system using SVM and KNN classifier", In: *Proc. of 2017*

International Conference on Inventive Systems and Control (ICISC), 2017

- [21] K. Chen, D. Zhang, L. Yao, B. Guo, Z. Yu, and Y. Liu, “Deep Learning for Sensor-based Human Activity Recognition”, *ACM Computing Surveys*, Vol. 54, No. 4, pp. 1–40, 2022.
- [22] A. Hayat, F. Morgado-Dias, B. Bhuyan, and R. Tomar, “Human Activity Recognition for Elderly People Using Machine and Deep Learning Approaches”, *Information*, Vol. 13, No. 6, pp. 275, 2022.
- [23] D. He, S. Chan, and M. Guizani, “User privacy and data trustworthiness in mobile crowd sensing”, *IEEE Wireless Communications*, Vol. 22, No. 1, pp. 28–34, 2015.
- [24] D. Zhang, L. Wang, H. Xiong, and B. Guo, “4W1H in mobile crowd sensing”, *IEEE Communications Magazine*, Vol. 52, No. 8, pp. 42–48, 2014.
- [25] N. P. Owoh and M. M. Singh, “Security analysis of mobile crowd sensing applications”, *Applied Computing and Informatics*, Vol. 18, No. 1/2, pp. 2–21, 2022.
- [26] L. Xiao, D. Jiang, D. Xu, W. Su, N. An, and D. Wang, “Secure mobile crowdsensing based on deep learning”, *China Communications*, Vol. 15, No. 10, pp. 1–11, 2018.
- [27] Y. Zhang and B. Kantarci, “Invited Paper: AI-Based Security Design of Mobile Crowdsensing Systems: Review, Challenges and Case Studies”, In: *Proc. of 2019 IEEE International Conference on Service-Oriented System Engineering (SOSE)*, pp. 17–1709, 2019.
- [28] T. Chen and C. Guestrin, “XGBoost”, In: *Proc. of the 22nd ACM SIGKDD International Conference on Knowledge Discovery and Data Mining*, New York, USA, pp. 785–794, 2016.
- [29] D. Tao, Y. Wen, and R. Hong, “Multicolumn Bidirectional Long Short-Term Memory for Mobile Devices-Based Human Activity Recognition”, *IEEE Internet Things J*, Vol. 3, No. 6, pp. 1124–1134, 2016.
- [30] F. Li, M. Al-qaness, Y. Zhang, B. Zhao, and X. Luan, “A Robust and Device-Free System for the Recognition and Classification of Elderly Activities”, *Sensors*, Vol. 16, No. 12, pp. 2043, 2016.
- [31] M. Tao, X. Li, W. Wei, and H. Yuan, “Jointly optimization for activity recognition in secure IoT-enabled elderly care applications”, *Applied Soft Computing*, Vol. 99, pp. 106788, 2021.
- [32] G. Csizmadia, K. L. Peres, B. Ferdinandy, Á. Miklósi, and V. Konok, “Human activity recognition of children with wearable devices using LightGBM machine learning”, *Scientific Reports*, Vol. 12, No. 1, pp. 5472, 2022.
- [33] G. Ke, Q. Meng, T. Finley, T. Wang, W. Chen, W. Ma, Q. ye, T. Y. Liu, “LightGBM: a highly efficient gradient boosting decision tree”, In: *NIPS’17: Proc. of the 31st International Conference on Neural Information Processing Systems*, pp. 3149–3157, 2017.
- [34] X. Gao, H. Luo, Q. Wang, F. Zhao, L. Ye, and Y. Zhang, “A Human Activity Recognition Algorithm Based on Stacking Denoising Autoencoder and LightGBM”, *Sensors*, Vol. 19, No. 4, p. 947, 2019.
- [35] Y. Zhang, X. Zhao, and Z. Li, “Facilitated and Enhanced Human Activity Recognition via Semi-supervised LightGBM”, In: *Proc. of 2020 IEEE Globecom Workshops (GC Wkshps)*, IEEE, pp. 1–6, 2020.
- [36] D. Powers and Ailab, “Evaluation: From precision, recall and F-measure to ROC, informedness, markedness & correlation”, *Journal of Machine Learning Technologies* Vol. 2, pp. 2229–3981, 2011.